Quantum critical behavior in disordered itinerant ferromagnets: Logarithmic corrections to scaling

D. Belitz
Department of Physics and Materials Science Institute, University of Oregon, Eugene, Oregon 97403

T. R. Kirkpatrick
Institute for Physical Science and Technology and Department of Physics, University of Maryland, College Park, Maryland 20742

Maria Teresa Mercaldo
Institute for Physical Science and Technology, and Department of Physics, University of Maryland, College Park, Maryland 20742 and Dipartimento di Scienze Fisiche ''E. R. Caianiello'' and Istituto Nazionale di Fisica per la Materia, Universitá di Salerno, I-84081 Baronissi, Salerno, Italy

Sharon L. Sessions
Department of Physics and Materials Science Institute, University of Oregon, Eugene, Oregon 97403
(Received 26 October 2000; published 11 April 2001)

The quantum critical behavior of disordered itinerant ferromagnets is determined exactly by solving a recently developed effective field theory. It is shown that there are logarithmic corrections to a previous calculation of the critical behavior, and that the exact critical behavior coincides with that found earlier for a phase transition of undetermined nature in disordered interacting-electron systems. This confirms a previous suggestion that the unspecified transition should be identified with the ferromagnetic transition. The behavior of the conductivity, the tunneling density of states, and the phase and quasiparticle-relaxation rates across the ferromagnetic transition are also calculated.

DOI: 10.1103/PhysRevB.63.174428 PACS number(s): 75.20.En, 75.10.Lp, 75.40.Cx, 75.40.Gb

I. INTRODUCTION

In a recent paper,[1] hereafter denoted by I, a local field theory capable of describing the zero-temperature ($T=0$) ferromagnetic phase transition in disordered itinerant electron systems was developed. In the present paper this theory is used to exactly determine the critical behavior at the phase transition and the connections between the local theory and previous descriptions of the ferromagnetic quantum phase transition are established.

Historically, the ferromagnetic transition in itinerant electron systems at $T=0$ was the first quantum phase transition to be studied in detail. Hertz[2] concluded that the transition in the physically interesting dimension $d=3$ was mean-field-like. The basic idea behind this result was that the effective dimension of the system, which is given by the spatial dimension d plus the effective time dimension z, was above the upper-critical dimension for the transition so that fluctuation effects could be ignored. This conclusion is now known to be incorrect. For example, the Harris criterion[3] for phase transitions in disordered systems states that the correlation-length exponent ν must satisfy the inequality $\nu \geqslant 2/d$, whereas the mean-field theory gives $\nu=1/2$ for all d. This in turn implies that a simple mean-field description *must* break down in dimensions $d<4$.

The reason for this breakdown of the mean-field theory was shown in Ref. 4 to be the existence, in itinerant-electron systems, of soft or massless modes other than the order parameter fluctuations, which were not taken into account in Hertz's theory. In disordered systems these modes are diffusive and they couple to the order-parameter fluctuations and modify the critical behavior.[5] Among other things, they lead to a correlation-length exponent that satisfies the Harris criterion. Technically, if these additional soft modes are integrated out, they lead to a long-ranged interaction between the order-parameter fluctuations. It was argued that once this effect is taken into account, all other fluctuation effects are suppressed by the long-range nature of the interactions, and that the critical behavior is governed by a fixed point that is Gaussian but does not yield mean-field exponents. It was thought that the critical behavior found in Ref. 4 was exact.

Several years before the work reported in Ref. 4, the study of metal-insulator transitions of disordered interacting electrons constituted a separate development in the many-electron problem.[7] Within this context, a transition was encountered that was *not* a metal-insulator transition but rather of magnetic nature.[8] Due to the methods used in Ref. 8, the order parameter and the nature of the ordered state were not identified, but the critical behavior was determined and was found to consist of power laws with simple exponents modified by complicated logarithmic corrections. The critical behavior for the ferromagnetic transition determined in Ref. 4 turned out to consist of the same simple power laws albeit with different and much simpler logarithmic corrections. This led, in Ref. 4, to the suggestion that the transition studied in Ref. 8 was in fact the ferromagnetic transition. The discrepancy in the logarithmic corrections between the two approaches was attributed to the fact that of the two integral equations derived in Ref. 8, only one had been shown to be exact. The conclusion thus was that the theories presented in Refs. 4 and 8 had treated the same problem, and that the former solution was exact while the latter was approximate.

The latter conclusion, however, relied on a weak link in

the chain of arguments since the theory developed in Ref. 4 was not very suitable for determining logarithmic corrections to power laws. The reason was that the additional soft modes were integrated out to obtain a description solely in terms of order-parameter fluctuations. The resulting field theory was thus nonlocal, which makes explicit calculations cumbersome. Consequently, most of the arguments used in Ref. 4 to determine the critical behavior were simple power-counting techniques that were not sensitive to logarithmic corrections to power laws.

It is the purpose of the present paper, in conjunction with the preceding paper, to settle the remaining questions regarding the relation between Refs. 4 and 8, and the exact critical behavior, including logarithmic corrections to scaling at the quantum ferromagnetic transition of disordered itinerant electrons. By using the local field-theoretic description of I that explicitly keeps all soft modes, we show that Ref. 4 missed marginal operators that lead to logarithmic corrections to the Gaussian critical behavior discussed there. Moreover, taking these marginal operators into account leads to integral equations for the relevant vertex functions that are identical to the ones derived in Ref. 8. The current formulation can further be mapped onto the one of Ref. 8, which shows that the transition found in the latter paper was really the ferromagnetic one, and that the results originally derived in that reference are exact.

This paper is organized as follows. In Sec. II we first recall the results of I. We then use diagrammatic techniques to derive exact integral equations for the two-point vertex functions that appear in the theory. We conclude this section by quoting a previous solution to these equations that is valid at the critical point. In Sec. III we show how some physical observables in the paramagnetic phase are related to these vertex functions. We then develop a scaling theory to determine the critical behavior of other observables of interest as well as the critical behavior in the ferromagnetic phase. In Sec. IV we discuss general theoretical aspects of this paper as well as experimental consequences of our results. Various technical issues are relegated to several appendices.

II. EFFECTIVE FIELD THEORY AND ITS SOLUTION

A. Effective action

In I it was shown that the effective long-wavelength and low-frequency field theory that contains the critical fixed point and describes the exact quantum critical behavior of disordered itinerant ferromagnets is given by the action

$$
\begin{aligned}
\mathcal{A}_{\rm eff} = & -\sum_{\mathbf{k},n,\alpha}\sum_{i=1}^{3} {}^{i}M_{n}^{\alpha}(\mathbf{k})u_{2}(\mathbf{k}){}^{i}M_{-n}^{\alpha}(-\mathbf{k}) - \frac{4}{G}\sum_{\mathbf{k}}\sum_{1,2,3,4}\sum_{r,i} {}_{r}^{i}q_{12}(\mathbf{k})\Gamma_{12,34}^{(2)}(\mathbf{k}){}_{r}^{i}q_{34}(-\mathbf{k}) \\
& - \frac{1}{4G}\sum_{1,2,3,4}\sum_{r,s,t,u}\sum_{i_1,i_2,i_3,i_4}\frac{1}{V}\sum_{\mathbf{k}_1,\mathbf{k}_2,\mathbf{k}_3,\mathbf{k}_4} {}_{rstu}^{i_1 i_2 i_3 i_4}\Gamma_{1234}^{(4)}(\mathbf{k}_1,\mathbf{k}_2,\mathbf{k}_3,\mathbf{k}_4){}_{r}^{i_1}q_{12}(\mathbf{k}_1){}_{s}^{i_2}q_{32}(\mathbf{k}_2){}_{t}^{i_3}q_{34}(\mathbf{k}_3){}_{u}^{i_4}q_{14}(\mathbf{k}_4) \\
& + c_1\sqrt{T}\sum_{\mathbf{k}}\sum_{12}\sum_{i,r} {}_{r}^{i}b_{12}(\mathbf{k}){}_{r}^{i}q_{12}(-\mathbf{k}) + c_2\sqrt{T}\frac{1}{\sqrt{V}}\sum_{\mathbf{k},\mathbf{p}}\sum_{n_1,n_2,m}\sum_{r,s,t}\sum_{i=1}^{3}\sum_{j,k}\sum_{\alpha,\beta} {}_{r}^{i}b_{n_1 n_2}^{\alpha\alpha}(\mathbf{k}) \\
& \times[{}_{s}^{j}q_{n_2 m}^{\alpha\beta}(\mathbf{p}){}_{t}^{k}q_{n_1 m}^{\alpha\beta}(-\mathbf{p}-\mathbf{k})\mathrm{tr}(\tau_r\tau_s\tau_t^{\dagger})\mathrm{tr}(s_i s_j s_k^{\dagger}) - {}_{s}^{j}q_{m n_2}^{\beta\alpha}(\mathbf{p}){}_{t}^{k}q_{m n_1}^{\beta\alpha}(-\mathbf{p}-\mathbf{k})\mathrm{tr}(\tau_r\tau_s^{\dagger}\tau_t)\mathrm{tr}(s_i s_j^{\dagger}s_k)]. \qquad (2.1)
\end{aligned}
$$

Here $\mathbf{M}_n^{\alpha}(\mathbf{k})$, with components ${}^{i}M_n^{\alpha}(\mathbf{k})$, is the fluctuating magnetization at wavenumber $\mathbf{k}$ and bosonic Matsubara frequency $\Omega_n = 2\pi T n$, where α is a replica label and the field b is defined in terms of the magnetization,

$$
{}_{r}^{i}b_{12}(\mathbf{k}) = \delta_{\alpha_1\alpha_2}(-)^{r/2}\sum_{n}\delta_{n,n_1-n_2} \times[{}^{i}M_{n}^{\alpha_1}(\mathbf{k}) + (-)^{r+1\,i}M_{-n}^{\alpha_1}(\mathbf{k})]. \qquad (2.2)
$$

The labels 1, 2, etc., comprise both frequency and replica indices, $1 \equiv (n_1, \alpha_1)$, etc. The two-point M vertex is given by

$$
u_2(\mathbf{k}) = t_0 + a_{d-2}|\mathbf{k}|^{d-2} + a_2\mathbf{k}^2. \qquad (2.3a)
$$

Here the nonanalytic term proportional to $|\mathbf{k}|^{d-2}$ reflects the nonanalytic wavenumber dependence of the electron spin susceptibility in a disordered itinerant electron system, as has been explained in I. For weak disorder characterized by a mean-free path $l \gg 1/k_{\rm F}$, where $k_{\rm F}$ is the Fermi wavenumber, the prefactor a_{d-2} is of order $1/k_{\rm F}l$ while $a_2 = O(1)$. For physical values of the spatial dimension d and for asymptotically small wavenumbers, the nonanalytic term dominates the analytic $\mathbf{k}^2$ term. However, for completeness and later reference we include the latter, which had been dropped from the final effective action in I. t_0 is the bare distance from the ferromagnetic critical point.

The fermionic degrees of freedom are represented by the field q; electron number, spin, and energy-density fluctuations can all be expressed in terms of the ${}_{r}^{i}q_{nm}^{\alpha\beta}$. These are the additional slow modes mentioned in Sec. I above. The frequency labels $n \geq 0$, $m < 0$ of the q denote fermionic Matsubara frequency indices, i is a spin label ($i = 0$ and $i = 1,2,3$ correspond to spin-singlet and spin-triplet fluctuations, respectively), and the label r ($r = 0,3$) serves to write the complex-valued q fields as two-component real-number

valued fields.[9] The fermionic part of the action is characterized by the two-point vertex

$$\Gamma^{(2)}_{12,34}(\mathbf{k}) = \delta_{13}\delta_{24}(\mathbf{k}^2 + GH\Omega_{n_1-n_2}), \tag{2.3b}$$

and the four-point vertex

$$\begin{aligned}{}^{i_1 i_2 i_3 i_4}_{rstu}\Gamma^{(4)}_{1234}(\mathbf{k}_1,\mathbf{k}_2,\mathbf{k}_3,\mathbf{k}_4) &= -\delta_{\mathbf{k}_1+\mathbf{k}_2+\mathbf{k}_3+\mathbf{k}_4,0}\,\mathrm{tr}(\tau_r\tau_s^\dagger\tau_t\tau_u^\dagger)\mathrm{tr}(s_{i_1}s_{i_2}^\dagger s_{i_3}s_{i_4}^\dagger)\\ &\times(\mathbf{k}_1\cdot\mathbf{k}_3+\mathbf{k}_1\cdot\mathbf{k}_4+\mathbf{k}_1\cdot\mathbf{k}_2+\mathbf{k}_2\cdot\mathbf{k}_4-GH\Omega_{n_1-n_2}).\end{aligned} \tag{2.3c}$$

The parameter $G=8/\pi\sigma_0$ is a measure of the disorder, where σ_0 is the bare conductivity. $H=\pi N_F/4$, where N_F is the bare single-particle or tunneling density of states per spin at the Fermi surface, is a bare quasiparticle density of states that also determines the specific-heat coefficient. Finally, c_1, c_2 are coupling constants whose bare values are related and given by

$$c_1 = 16c_2 = 4\sqrt{\pi K_t}, \tag{2.3d}$$

where K_t is the spin-triplet interaction amplitude of the electrons. The replicated partition function is given in terms of the action by

$$Z = \int D[\mathbf{M},q]e^{A_{\mathrm{eff}}[\mathbf{M},q]}. \tag{2.4}$$

B. Perturbation theory to all orders

We will now show that the effective action given in the preceding subsection can be solved perturbatively exactly, i.e., it is possible to resum perturbation theory to all orders. The basic idea is to first show that the n-point vertices for $n\geqslant 3$ are either not renormalized or their renormalization is simply related to that of the two-point vertex functions. This in turn implies that exact self-consistent equations for the two-point vertex functions can be derived. The net result will be that the determination of the critical behavior of the field theory is reduced to the solution of two coupled integral equations that were first derived by different methods in Ref. 8.

1. Gaussian propagators

In order to set up a loop expansion we will need the basic two-point propagators for the above theory. They are determined by the Gaussian action,

$$\begin{aligned}\mathcal{A}_G[\mathbf{M},q] = &-\sum_{\mathbf{k}}\sum_{n}\sum_{\alpha}\sum_{i=1}^{3}{}^{i}M_n^{\alpha}(\mathbf{k})u_2(\mathbf{k})^{i}M_{-n}^{\alpha}(-\mathbf{k})\\ &-\frac{4}{G}\sum_{\mathbf{k}}\sum_{1,2,3,4}\sum_{i,r}{}^{i}_{r}q_{12}(\mathbf{k})\Gamma^{(2)}_{12,34}(\mathbf{k})^{i}_{r}q_{34}(-\mathbf{k})\\ &+4\sqrt{\pi TK_t}\sum_{\mathbf{k}}\sum_{12}\sum_{i,r}{}^{i}_{r}q_{12}(\mathbf{k})^{i}_{r}b_{12}(-\mathbf{k}).\end{aligned} \tag{2.5}$$

The quadratic form defined by this Gaussian action has been inverted in I. For the order-parameter correlations we find

$$\langle {}^{i}M_n^{\alpha}(\mathbf{k})^{j}M_m^{\beta}(\mathbf{p})\rangle = \delta_{\mathbf{k},-\mathbf{p}}\delta_{n,-m}\delta_{ij}\delta_{\alpha\beta}\frac{1}{2}\mathcal{M}_n(\mathbf{k}), \tag{2.6a}$$

$$\langle {}^{i}_{r}b_{12}(\mathbf{k})^{j}_{s}b_{34}(\mathbf{p})\rangle = -\delta_{\mathbf{k},-\mathbf{p}}\delta_{rs}\delta_{ij}\delta_{\alpha_1\alpha_2}\delta_{\alpha_1\alpha_3}\mathcal{M}_{n_1-n_2}(\mathbf{k})\times[\delta_{1-2,3-4}-(-)^{r}\delta_{1-2,4-3}]; \tag{2.6b}$$

in terms of the paramagnon propagator,

$$\mathcal{M}_n(\mathbf{k}) = \frac{1}{t_0 + a_{d-2}|\mathbf{k}|^{d-2} + a_2\mathbf{k}^2 + \dfrac{GK_t|\Omega_n|}{\mathbf{k}^2+GH|\Omega_n|}}. \tag{2.6c}$$

The dynamical piece of the paramagnon propagator $\mathcal{M}$, whose structure is characteristic of disordered itinerant ferromagnets, has been produced by the coupling between the order-parameter field and the fermionic degrees of freedom.

For the fermionic propagators one finds

$$\langle {}^{i}_{r}q_{12}(\mathbf{k})^{j}_{s}q_{34}(\mathbf{p})\rangle = \delta_{\mathbf{k},-\mathbf{p}}\delta_{rs}\delta_{ij}\frac{G}{8}{}^{i}\Gamma^{(2)-1}_{12,34}(\mathbf{k}); \tag{2.7}$$

in terms of the inverse of $\Gamma^{(2)}$,

$${}^{0}\Gamma^{(2)-1}_{12,34}(\mathbf{k}) = \delta_{13}\delta_{24}\mathcal{D}_{n_1-n_2}(\mathbf{k}), \tag{2.8a}$$

and the propagator

$$\begin{aligned}{}^{1,2,3}\Gamma^{(2)-1}_{12,34}(\mathbf{k}) = &\delta_{13}\delta_{24}\mathcal{D}_{n_1-n_2}(\mathbf{k})\\ &-\delta_{1-2,3-4}\delta_{\alpha_1\alpha_2}\delta_{\alpha_1\alpha_3}2\pi TGK_t\\ &\times[\mathcal{D}_{n_1-n_2}(\mathbf{k})]^2\mathcal{M}_{n_1-n_2}(\mathbf{k}).\end{aligned} \tag{2.8b}$$

Here $\mathcal{D}$ is the basic diffusion propagator or diffusion. In the limit of small frequencies and wave numbers it reads

$$\mathcal{D}_n(\mathbf{k}) = \frac{1}{\mathbf{k}^2 + GH\Omega_n}. \tag{2.9}$$

Physically, $\mathcal{D}$ describes heat diffusion.[10,7]

Finally, due to the coupling between M and q there is a mixed propagator,

$$\begin{aligned}\langle {}^{i}_{r}q_{12}(\mathbf{k})^{j}_{s}b_{34}(\mathbf{p})\rangle = &-\delta_{\mathbf{k},-\mathbf{p}}\delta_{rs}\delta_{ij}\delta_{\alpha_1\alpha_2}\delta_{\alpha_1\alpha_3}\\ &\times\frac{G}{2}\sqrt{\pi TK_t}\mathcal{D}_{n_1-n_2}(\mathbf{k})\mathcal{M}_{n_1-n_2}(\mathbf{k})\\ &\times[\delta_{1-2,3-4}+(-)^{r+1}\delta_{1-2,4-3}].\end{aligned} \tag{2.10}$$

2. Three-point and four-point vertices

We now determine loop corrections to the tree-level theory. We begin by considering the three-point vertex whose coupling constant is denoted by c_2 in Eq. (2.1). Dia-

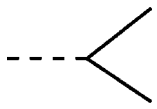

FIG. 1. Diagrammatic representation of the bare bq^2 vertex. Dashed lines denote M or b fields and solid lines denote q fields.

grammatically the bare three-point vertex is given in Fig. 1. Now consider the one-loop renormalizations of this vertex, which are shown in Fig. 2.

For scaling purposes we can use simple estimates for the propagators. Specifically, the q propagators all scale like an inverse wavenumber squared,[11]

$$\langle q_{12}(\mathbf{k})q_{34}(-\mathbf{k})\rangle \sim 1/\mathbf{k}^2. \tag{2.11a}$$

The M propagator at criticality may scale like a number or like an inverse wave number to the power $d-2$. This depends on the scaling behavior of the frequency, which can be different in different contexts as has been explained in I and can be seen from Eqs. (2.6c) and (2.9), respectively: Ω can scale either like $|\mathbf{k}|^d$ as in the paramagnon propagator or like $\mathbf{k}^2$ as in the diffusion. The two possibilities therefore are

$$\langle M_1(\mathbf{k})M_2(-\mathbf{k})\rangle \sim \begin{cases} \text{const} & \text{if } \Omega \sim \mathbf{k}^2 \\ 1/|\mathbf{k}|^{d-2} & \text{if } \Omega \sim |\mathbf{k}|^d. \end{cases} \tag{2.11b}$$

Similarly, the mixed propagator, Eq. (2.10), scales like

$$\langle q_{12}(\mathbf{k})b_{34}(-\mathbf{k})\rangle \sim \begin{cases} 1/|\mathbf{k}| & \text{if } \Omega \sim \mathbf{k}^2 \\ 1/|\mathbf{k}|^{d/2} & \text{if } \Omega \sim |\mathbf{k}|^d. \end{cases} \tag{2.11c}$$

If we use an infrared wave number cutoff Λ, we see that the integrals that correspond to the diagrams shown in Fig. 2 all scale like Λ^{d-2}. That is, the one-loop renormalization of c_2 at zero external wave number and frequency is a finite number for all $d>2$. More generally, an n-loop skeleton diagram has n independent wave number and frequency integrals. Diagrams that contain only solid and dashed lines contain $2n$ $\langle qq\rangle$ propagators and up to n $\langle MM\rangle$ propagators. Similar considerations hold for diagrams that contain mixed propagators. The net result is that any n-loop skeleton diagram scales like $\Lambda^{n(d-2)}$. All of these contributions thus amount to finite corrections to the bare value of c_2. By induction it follows that insertions do not produce singular contributions either. We conclude that there are no singular renormalizations of the three-point vertex function in the field theory defined by Eq. (2.1).

In addition to the renormalization of c_2, a new three-point vertex with a replica structure that is different from the one

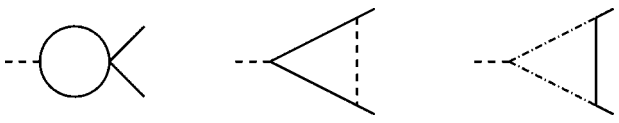

FIG. 2. One-loop corrections to the vertex shown in Fig. 1. Solid lines denote $\langle qq\rangle$ propagators, dashed lines denote $\langle bb\rangle$ propagators, and dashed-dotted lines denote $\langle bq\rangle$ propagators.

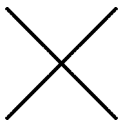

FIG. 3. The bare four-point vertex.

of c_2 is generated by the renormalization group at one-loop order. As shown in Appendix A, the frequency structure of this vertex is such that it carries one more frequency sum and associated temperature factor than the vertex with coupling constant c_2. Its coupling constant is therefore more irrelevant than c_2 and can be neglected.

Next we consider the four-point vertex $\Gamma^{(4)}$ in Eq. (2.1). The bare four-point vertex is given analytically in Eq. (2.3c) and shown diagrammatically in Fig. 3, and the one-loop renormalizations are shown in Fig. 4.

Notice that this vertex is proportional either to a wave number squared or to a frequency. Using the estimates given by Eqs. (2.11), we find that the renormalization of the part of $\Gamma^{(4)}$ that is proportional to a wave number squared is always a finite number again scaling as $\Lambda^{(d-2)}$. For the part that is proportional to frequency, on the other hand, power counting shows that this term can have logarithmically singular renormalizations. An explicit calculation would be very cumbersome. However, it is not necessary since the one-loop renormalization of the coupling constant H in Eq. (2.3c) obtained this way is identical to that obtained by renormalizing the two-point vertex, Eq. (2.3b). This is because both terms arise from the same term in the underlying nonlinear sigma model for the fermionic degrees of freedom, which is believed to be renormalizable.[12] By the same argument, the renormalization of $\Gamma^{(4)}$ to *all orders* is given by that of $\Gamma^{(2)}$ and therefore need not be considered separately. The explicit calculation of $\Gamma^{(2)}$ confirms the existence of the logarithms that were alluded to above as we will demonstrate in the next subsection.

In addition to the diagrams that renormalize $\Gamma^{(4)}$, there are one-loop terms that represent four-point vertices with more restrictive replica structures. These correspond either to the two-body interaction terms that were shown in I to not change the critical behavior, or to many-body interactions that are shown in Appendix A to be more irrelevant than $\Gamma^{(4)}$ and thus can be neglected.

3. Two-point vertices

We now turn to the two-point vertices in the effective action. The one-loop renormalization of the bq vertex is shown in Fig. 5.

Using Eqs. (2.11), it is easy to see that this diagram is finite in $d>2$. Since the three-point vertex is not singularly renormalized, see the previous subsection, it follows that the bq vertex has only finite renormalizations to all orders in perturbation theory. This means that the coupling constant K_t

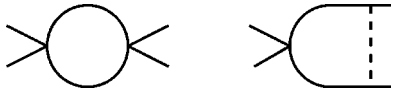

FIG. 4. One-loop corrections to the vertex shown in Fig. 3.

FIG. 5. One-loop renormalizations of the mixed two-point vertex.

is not singularly renormalized.

The one-loop renormalizations of $\Gamma^{(2)}$ are shown in Fig. 6.

As was shown in I, the renormalization of G obtained from these diagrams is finite in $d>2$. For the renormalized H, which we denote by $H(i\Omega_n)$, one obtains to one-loop order

$$H(i\Omega_n)=H+\frac{3}{8}GK_t\frac{2\pi T}{\Omega_n}\sum_{l=0}^{n}\frac{1}{V}\sum_{\mathbf{p}}\mathcal{D}_l(\mathbf{p})\mathcal{M}_l(\mathbf{p}), \tag{2.12}$$

which diverges logarithmically as $\Omega_n\to 0$ for all $2<d<4$. As was explained in I, this divergent renormalization, which arises from the nominally irrelevant vertices $\Gamma^{(4)}$ and c_2, is a consequence of the presence of two time scales in the problem. In addition, there are terms that are finite in $d>2$. It is important to note that the structure $\mathcal{DM}$ in the integrand of Eq. (2.12) stems from the second term proportional to $\mathcal{D}^2\mathcal{M}$ in the triplet qq propagator, Eq. (2.8b), times a term $\mathcal{D}^{-1}$ that is due to the wave number and frequency dependence of the quartic vertex, Eq. (2.3c).

The exact vertex $\Gamma^{(2)}$ can be generated from the one-loop diagrams by dressing all propagators and all vertices in Fig. 6. The relevant vertices are $\Gamma^{(4)}$ and c_2. As was shown in Sec. II B 2, the latter has no singular renormalizations in $d>2$ so it need not be dressed. Denoting the exact four-q vertex by a square and the dressed propagators by double lines, we therefore have the diagrammatic representation of the renormalization of $\Gamma^{(2)}$ to *all orders* shown in Fig. 7.

Analytically, this result corresponds to simply dressing the propagators in Eq. (2.12). Notice that this procedure includes the vertex renormalization due to the structure pointed out above. Also notice that it is crucial for our argument that G and K_t carry finite renormalizations only. We thus have the exact result, as far as the asymptotic critical behavior is concerned,

$$H(i\Omega_n)=H+\frac{3}{8}GK_t\frac{2\pi T}{\Omega_n}\sum_{l=0}^{n}\frac{1}{V}\times\sum_{\mathbf{p}}\frac{1}{GK_t\Omega_l+\mathbf{p}^2u_2(\mathbf{p},i\Omega_l)}, \tag{2.13a}$$

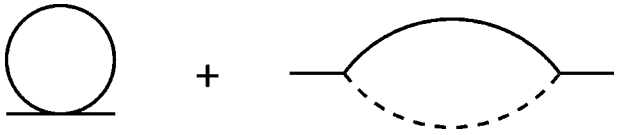

FIG. 6. One-loop renormalizations of the fermionic two-point vertex $\Gamma^{(2)}$.

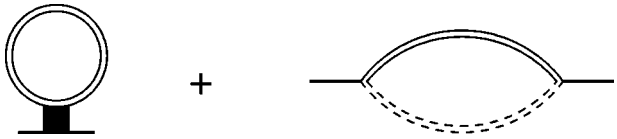

FIG. 7. Renormalization of the fermionic two-point vertex $\Gamma^{(2)}$ to all orders.

where $u_2(\mathbf{p},i\Omega_l)$ is the fully renormalized bb vertex. By the same arguments, we obtain the latter as shown in Fig. 8. By dressing the propagators in the analytic one-loop expression given in Eq. (3.5b) of I, we have for $\Omega_n\geqslant 0$,

$$u_2(\mathbf{k},i\Omega_n)=t_0-\frac{G^2}{2}\frac{K_t}{V}\sum_{\mathbf{p}}2\pi T\times\sum_{l=0}^{\infty}\frac{1}{\mathbf{p}^2+GH(i\Omega_l)\Omega_l}\times\frac{1}{(\mathbf{p}+\mathbf{k})^2+GH(i\Omega_l+i\Omega_n)(\Omega_l+\Omega_n)}. \tag{2.13b}$$

In writing Eq. (2.13b), we have for simplicity put the bare coupling constants a_{d-2} and a_2 equal to zero since they are generated at one-loop order.

C. Integral equations for diffusion coefficients

Equation (2.13) in Sec. II B constitute two closed integral equations for the two-point vertices. As we have seen, this has been possible to achieve since (1) the four-point vertex $\Gamma^{(4)}$ renormalizes like the two-point vertex $\Gamma^{(2)}$ and (2) all other vertices are subject to finite renormalizations only. As a result, the solution of Eqs. (2.13) provides us with the perturbatively *exact* critical behavior.

To make contact with previous work, it is useful to rewrite Eqs. (2.13) in terms of the (thermal) diffusion coefficient $D(i\Omega_n)=1/GH(i\Omega_n)$ and the spin diffusion coefficient, $D_s(\mathbf{k},i\Omega_n)=u_2(\mathbf{k},i\Omega_n)/GK_t$. If we analytically continue to real frequencies, $i\Omega_n\to\Omega+i0$, the self-consistent one-loop equations read

$$D_s(\mathbf{k},\Omega)=D_s^0+\frac{iG}{2V}\sum_{\mathbf{p}}\int_0^\infty d\omega\times\frac{1}{\mathbf{p}^2-i\omega/D(\omega)}\frac{1}{(\mathbf{p}+\mathbf{k})^2-i(\omega+\Omega)/D(\omega+\Omega)}, \tag{2.14a}$$

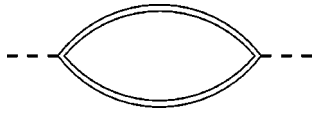

FIG. 8. Renormalization of the two-point magnetization vertex u_2 to all orders.

$$\frac{1}{D(\Omega)} = \frac{1}{D^0} + \frac{3G}{8V}\sum_{\mathbf{p}}\frac{1}{\Omega}\int_0^\Omega d\omega \frac{1}{-i\omega + \mathbf{p}^2 D_s(\mathbf{p},\omega)}. \tag{2.14b}$$

Here $D^0 = 1/GH$ and $D_s^0 = t_0/GK_t$ are the bare diffusion coefficients. These integral equations were first derived in Ref. 8 by means of a resummation of perturbation theory within a nonlinear sigma model for interacting electrons in the limit of a large spin-triplet interaction amplitude. As has been discussed in I, this sigma model is recovered from the current model by integrating out the magnetization. This is the mapping between the two models that was referred to in the Introduction.

D. Solution of the integral equations

In Ref. 8 the coupled integral equations, Eqs. (2.14), were solved by three distinct methods: a direct analytic solution, a renormalization group (RG) solution, and a numerical solution. The results of all three approaches were consistent with one another. Here we will quote the most relevant results restricting ourselves as in I to $2<d<4$.

Simple scaling arguments show that at criticality, $t \equiv u_2(\mathbf{k}=0,\Omega_n=0)=0$, $D(\Omega\to 0)$ is a constant except for logarithmic terms. This suggests the ansatz

$$D(\Omega) = D^0/F[\ln(1/\Omega\tau)]. \tag{2.15}$$

Here $1/\tau = \pi nG/8m$, where n is the electron density and m is the electron effective mass, is the elastic-scattering rate. The same arguments yield $D_s(\mathbf{k},\Omega=0)\sim|\mathbf{k}|^{d-2}$ at the critical point except for logarithmic terms. So we write

$$D_s(\mathbf{k},\Omega=0) = D_s^0(|\mathbf{k}|/k_F)^{d-2}F_s[\ln(k_F/|\mathbf{k}|)]. \tag{2.16}$$

Solving the resulting equations for F and F_s gives[8]

$$D(\Omega\to 0) = D^0[g\{\ln 1/\Omega\tau)\}]^{-1}, \tag{2.17a}$$

$$D_s(\mathbf{k}\to 0,\Omega=0) = D_s^0(|\mathbf{k}|/k_F)^{d-2}d'(GK_t/H)k_F^{d-2} \times[g\{2\ln(k_F/|\mathbf{k}|)\}]^{-1}. \tag{2.17b}$$

Here

$$g(x) = \sum_{n=0}^{\infty}[\{c(d)x\}^n/n!]\exp[(n^2-n)\ln(2/d)/2]. \tag{2.18a}$$

In an asymptotic expansion for large x, the leading term is

$$g(x)\approx[2\ln(d/2)/\pi]^{-1/2}\exp([\ln\{c(d)x\}]^2/2\ln(d/2)). \tag{2.18b}$$

The dimensionality-dependent coefficient $c(d)$ is given by

$$c(d) = c'(d)/d'(d), \tag{2.19a}$$

where

$$d'(d) = c''\Gamma(2-d/2)F(2-d/2,1/2;3/2;1), \tag{2.19b}$$

where F is a hypergeometric function, Γ is the gamma function, and c' and c'' are smoothly varying functions of d.

The leading dependence of either D or D_s on t away from criticality at zero frequency and wave number or that of D_s at $t=0$ as a function of frequency at $\mathbf{k}=0$, will follow from the scaling theory to be developed in Sec. III below.

III. CRITICAL BEHAVIOR OF OBSERVABLES

In this section we determine the exact critical behavior of various observables. We do so by developing a general scaling description for the free energy and various transport coefficients and relaxation rates, and using the exact solution of Sec. II to determine the values of the independent critical exponents. Again, we restrict ourselves to the dimensionality range $2<d<4$. The results for $d>4$ in Ref. 4 were exact, and the behavior in $d=4$ can be obtained by combining the solution of the integral equations from Ref. 8 for that case with the arguments given below. We have also checked some of our results by means of explicit perturbation theory, see Appendix B. Parts of the results presented here have been previously published in Ref. 13.

A. Identification of observables

We first discuss how to relate the behavior of some physical observables of interest near the quantum critical point to the solution of the effective field theory given in Sec. II. We consider the electrical conductivity σ, the specific-heat coefficient γ_C, the tunneling density of states N, the spin susceptibility χ_s, the heat and spin diffusion coefficients D and D_s, respectively, the phase relaxation rate $\tau_{\rm ph}^{-1}$, and various quasiparticle properties, in particular, the quasiparticle decay rate $\tau_{\rm QP}^{-1}$. The magnetization m will be obtained from the free energy in Sec. III B below.

The conductivity, $\sigma = 8/\pi G = 1/\rho$, where is ρ the resistivity, is proportional to the inverse of the renormalized disorder parameter G in Eq. (2.1) and the specific-heat coefficient $\gamma_C = C/T$, where C is the specific heat, is proportional to the renormalized value of H in Eqs. (2.3b) and (2.3c).[7] The single-particle density of states (DOS) as a function of the distance in energy or frequency space from the Fermi surface $\mathrm{N}(\epsilon)$ is given by Eq. (2.29d) in I. In terms of expectation values of the field q, it takes the form of an expansion

$$N(\epsilon_F+\epsilon) = N_F\Bigg[1 - \frac{1}{2}\sum_\beta\sum_m\sum_{i,r}\langle {}^i_r q^{\alpha\beta}_{nm}(\mathbf{x})\,{}^i_r q^{\alpha\beta}_{nm}(\mathbf{x})\rangle_{i\omega_n\to\epsilon+i0} + O(\langle q^4\rangle)\Bigg]. \tag{3.1}$$

Experimentally, ϵ is equal to the electron-charge times the bias voltage. The dynamical spin susceptibility is given by the $\mathbf{M}\cdot\mathbf{M}$ correlation function and we have seen that the coupling between the $\mathbf{M}$ and q fields affects the dynamical part of that correlation function only. This implies that the static spin susceptibility $\chi_s(\mathbf{k})$ is given by the renormalized value of $u_2(\mathbf{k},i\Omega_n=0)$, compare Eq. (2.13b). Alternatively, it is proportional to the inverse of the static spin diffusion coefficient

$$\chi_s(\mathbf{k}) = \frac{1}{2GK_t D_s(\mathbf{k}, i\Omega_n = 0)}. \tag{3.2}$$

The heat and spin diffusion coefficients D and D_s are explicitly given by the solution of the integral equations discussed in Sec. II. In Appendix C we show how to generalize the integral equations to the ordered phase, so that the equation of state or the magnetization m, can be obtained. In Sec. III B we determine the magnetization by means of a scaling theory.

The relaxation rates are defined in terms of the diffusion whose bare propagator is given by Eq. (2.9). Its renormalized counterpart has the form

$$\mathcal{D}(\mathbf{k}, i\Omega_n) = \frac{Z^2}{\mathbf{k}^2 + GH(i\Omega_n)\Omega_n} = \frac{Z^2}{\mathbf{k}^2 + \Omega_n / D(i\Omega_n)}. \tag{3.3a}$$

Here Z is the wave function renormalization, which determines the single-particle DOS, Eq. (3.1), via $N = N_F Z$. In addition, the quasiparticle DOS N_{QP} is related to N via

$$N_{QP} = N / a_{QP}, \tag{3.3b}$$

where a_{QP} is the quasiparticle weight. Upon an analytic continuation to real frequencies, $H(i\Omega_n)$ acquires a real part H' and an imaginary part H'', $H(i\Omega_n \to \epsilon + i0) = H'(\epsilon) + iH''(\epsilon)$. Dividing by GH', the renormalized diffusion can be written

$$\mathcal{D}(\mathbf{k}, i\Omega_n \to \epsilon + i0) = \frac{1}{G} \frac{(N_{QP}/N_F^2) a_{QP}^2}{D_{QP}\mathbf{k}^2 - i\epsilon + \tau_{QP}^{-1}}, \tag{3.3c}$$

where $a_{QP} = N_F Z / H'(\epsilon)$, $N_{QP} = H'(\epsilon)$, $D_{QP} = 1/GH'(\epsilon)$ is the quasiparticle diffusion coefficient, and

$$\tau_{QP}^{-1} = \epsilon H''(\epsilon)/H'(\epsilon) \tag{3.4a}$$

is the quasiparticle decay rate. In contrast, the phase breaking rate τ_{ph}^{-1} is the ''mass'' that is acquired by the diffusion at real frequencies and finite temperature. Equation (3.3a) shows that it can be identified, apart from a multiplicative constant, with

$$\tau_{ph}^{-1} = \mathrm{Re}[\Omega H(i\Omega)]/N_F|_{i\Omega \to \epsilon + i0} \tag{3.4b}$$

or in terms of the imaginary part of H,

$$\tau_{ph}^{-1} = \epsilon H''(\epsilon)/N_F. \tag{3.4c}$$

For later reference we also give the renormalized paramagnon propagator. Leaving out terms that are irrelevant for our purposes, it reads

$$\mathcal{M}(\mathbf{k}, i\Omega_n) = \frac{1}{u_2(\mathbf{k}, i\Omega_n) + GK_t|\Omega_n|/\mathbf{k}^2} = \frac{1/GK_t}{D_s(\mathbf{k}, i\Omega_n) + |\Omega_n|/\mathbf{k}^2}. \tag{3.5}$$

The above quantities have all been defined at $T = 0$, with an eye on the fact that the results of Sec. II are only valid at $T = 0$. In general, we are also interested in the analogous results at $T > 0$. This is of particular importance for the relaxation rates, since only at $T > 0$ do they provide a mass for the diffusion propagator and hence constitute a true real-time decay rate. In order to obtain complete results at finite temperatures, a Matsubara frequency sum and an analytic continuation to real frequencies need to be performed. The leading temperature dependence of the inelastic-scattering rates actually comes from a branch cut in this analytic continuation.[14] It turns out that to capture this effect one needs to retain terms that were neglected in the derivation of the integral equations in Sec. II. Alternatively, the inelastic-scattering rates at $T = 0$ as functions of real frequency or the distance in energy space from the Fermi surface can be obtained from the results of Sec. II, see Eqs. (3.4) above. Scaling theory can then be used to obtain the results at $\epsilon = 0$ and $T > 0$. We will follow this second route.

B. Scaling considerations

In this section we develop a general scaling theory for the physical observables near the quantum critical point. The explicit solution given in Sec. II D is used to identify the results for the critical exponents.

1. Critical exponents

From the explicit solution quoted in Sec. II above, we obtain various critical exponents. As has been pointed out in I, there are multiple dynamical exponents. This is also obvious from Eqs. (2.14) in conjunction with Eqs. (2.17). Furthermore, the logarithmic corrections to scaling that characterize the solution of the field theory mean that the asymptotic critical behavior is not given by simple power laws. A convenient way to account for that is to write the critical behavior as power laws with scale-dependent critical exponents. For instance, the critical time scale, which determines the dynamics of the paramagnon propagator, is given by a dynamical exponent

$$z_c = d + \ln g(\ln b)/\ln b, \tag{3.6a}$$

where b is an arbitrary renormalization-group-length scale factor. To see this consider Eq. (3.5) in conjunction with Eq. (2.17b), which shows that the frequency in the paramagnon scales like $\Omega \sim \mathbf{k}^2 D_s(\mathbf{k}, \Omega = 0) \sim |\mathbf{k}|^d / g[\ln(k_F/|\mathbf{k}|)]$. In addition, there are diffusive time scales with power 2 and various logarithmic corrections. For instance, the frequency Ω in the dressed diffusion, Eq. (3.3a), defines a time scale with a critical exponent

$$\tilde{z}_d = 2 + \ln g(\ln b)/\ln b. \tag{3.6b}$$

There are other diffusive time scales, however. For instance, the quantity $H(i\Omega_n)\Omega_n/N_F$ is dimensionally a frequency that defines a time scale with critical exponent

$$z_d = 2. \tag{3.6c}$$

This is the scale dimension of the phase-relaxation rate, Eq. (3.4b). For the other two independent critical exponents we pick η, which describes the wave number dependence of the order-parameter susceptibility and the correlation-length exponent ν. From Eq. (2.17b), we have for the former

$$\eta = 4 - d - \ln g(\ln b)/\ln b. \tag{3.6d}$$

The exponent ν was determined in Ref. 8 with the result

$$1/\nu = d - 2 + \ln g(\ln b)/\ln b. \tag{3.6e}$$

The scale-dependent exponents shown determine the asymptotic critical behavior, including the leading logarithmic corrections to scaling. They do not include logarithmic terms that are less leading than the log-log-normal dependence due to the function $g(\ln b)$. In particular, simple powers of logarithms would correspond to terms of order $\ln\ln b/\ln b$ in Eqs. (3.6).

2. Thermodynamic quantities and the density of states

We start by considering the thermodynamic properties near the phase transition. They can all be obtained by a scaling ansatz for the free energy as a function of t, T, and h, where h is the magnetic field. Two key ideas will be used. First, the existence of two essentially different time scales, see Sec. III B 1, implies that the free-energy density f should consist of two scaling parts. The second idea is that h also represents an energy scale (namely, the Zeeman energy) and it therefore scales like the frequency or the temperature.

Taking all of this into account, the natural scaling ansatz for f is

$$f(t,T,h) = b^{-(d+z_c)} f_1(tb^{1/\nu}, Tb^{z_c}, hb^{z_c}) + b^{-(d+\tilde{z}_d)} f_2(tb^{1/\nu}, Tb^{\tilde{z}_d}, hb^{z_c}), \tag{3.7}$$

where f_1 and f_2 are scaling functions. Note that *a priori* there is no reason for the temperature argument of f_2 to be given by the diffusive time scale with the dynamical exponent $\tilde{z}_d$ rather than by the critical time scale with the dynamical exponent z_c. It requires explicit calculations to see that for some quantities, e.g., the magnetization, the diffusive temperature scale is the relevant one. In Appendix C we show that the equation of state contains only the diffusive temperature scale and our scaling ansatz for f_2 reflects this feature (see also Ref. 4). In addition to the T and h dependences in Eq. (3.7) with scales determined by z_c, there are subleading dependences involving the diffusive time scale that we suppress. The magnetization m, specific heat C, and spin susceptibility χ_s, respectively, are given by

$$m = \partial f/\partial h, \tag{3.8a}$$

$$C = -T\partial^2 f/\partial T^2, \tag{3.8b}$$

$$\chi_s = \partial^2 f/\partial h^2. \tag{3.8c}$$

Generalized homogeneity laws for m, $\gamma_C = C/T$ and χ_s are obtained by using Eq. (3.7) in Eqs. (3.8). Substituting the exponent values given by Eqs. (3.6), we find

$$m(t,T,h) = b^{-2} f_m(tb^{d-2} g(\ln b), Tb^2 g(\ln b), hb^d g(\ln b)), \tag{3.9a}$$

$$\gamma_C(t,T,h) = g(\ln b) f_\gamma(tb^{d-2} g(\ln b), Tb^d g(\ln b), hb^d g(\ln b)), \tag{3.9b}$$

$$\chi_s(t,T,h) = b^{d-2} g(\ln b) f_\chi(tb^{d-2} g(\ln b), Tb^2 g(\ln b), hb^d g(\ln b)), \tag{3.9c}$$

where f_m, f_γ, and f_χ are scaling functions. With suitable choices of the scale factor b, Eqs. (3.9) imply

$$m(t,0,0) = f_m(1,0,0)\left[tg\left(\frac{1}{d-2} \ln \frac{1}{t} \right) \right]^{2/(d-2)}, \tag{3.10a}$$

$$m(0,0,h) = f_m(0,0,1)\left[hg\left(\frac{1}{d} \ln \frac{1}{h} \right) \right]^{2/d}, \tag{3.10b}$$

$$\gamma_C(0,T,0) = f_\gamma(0,1,0) g\left(\frac{1}{d} \ln \frac{1}{T} \right), \tag{3.10c}$$

$$\chi_s(t,0,0) = f_\chi(1,0,0) t^{-1} \tag{3.10d}$$

for the leading asymptotic critical behavior in the sense explained at the end of Sec. III B 1. For the critical exponents β, γ, δ, and α, defined by $m \propto t^\beta$, $\chi_s \propto t^{-\gamma}$, $m \propto h^{1/\delta}$, and $\gamma_C \propto T^{-(1+\alpha)}$ (the latter is a generalization to zero-temperature transitions of the usual definition of the exponent α), we obtain from Eqs. (3.10)

$$\beta = 2\nu, \tag{3.11a}$$

$$\gamma = 1, \tag{3.11b}$$

$$\delta = z_c/2, \tag{3.11c}$$

$$\alpha = -d/z_c, \tag{3.11d}$$

with ν and z_c from Eqs. (3.6).

Next we consider the single-particle density of states. We define $\Delta N = N - N_F$, where N_F is the disordered Fermi-liquid value of N. ΔN can be related to a correlation function that has scale dimension $-(d-2)$.[15] This implies the scaling form

$$\Delta N(t,\epsilon,T) = b^{-(d-2)} f_N(tb^{d-2} g(\ln b), \epsilon b^d g(\ln b), Tb^d g(\ln b)). \tag{3.12a}$$

Notice that the scale dimension of ΔN is minus that of t, modulo the logarithmic corrections to the latter. This leads to a resonance in the RG-flow equations for ΔN, which in turn leads to an additional logarithmic dependence of ΔN on t, see Appendix D. Anticipating that logarithm, we generalize Eq. (3.12a) to

$$\Delta N(t,\epsilon,T) = \text{const}\times tg(\ln b)\ln b + b^{-(d-2)}\tilde{f}_N(tb^{d-2}g(\ln b), \epsilon b^d g(\ln b), Tb^d g(\ln b)). \quad (3.12b)$$

This implies

$$N(0,\epsilon,0) = N_F\left[1 + c_N\left\{\frac{\epsilon}{\epsilon_F}g\left(\frac{1}{d}\ln\frac{\epsilon_F}{\epsilon}\right)\right\}^{(d-2)/d} + O(\epsilon^{(d-2)/2})\right], \quad (3.13a)$$

and

$$N(t,0,0) = N_F\left[1 + d_N tg\left(\frac{1}{d-2}\ln\frac{1}{t}\right)\ln\frac{1}{t} + \cdots\right], \quad (3.13b)$$

with constants c_N and d_N. It should be pointed out, however, that one should not take the $tg(\ln 1/t)\ln t$ behavior in Eq. (3.13b) too seriously. The reason is that the log-log-normal factor $g(\ln 1/t)$ may have multiplicative simple-log corrections that the asymptotic solution of the field theory is not sensitive to, see the remark after Eq. (3.6e).

3. Transport coefficients

The scaling theory for the transport coefficients, σ, D, and D_s can be presented in several different ways. Here we give two arguments for the scaling part of σ. The first one starts with the fact that the conductivity is a charge-current correlation function whose scale dimension with respect to the quantum magnetic fixed point is expected to be zero. That is, σ neither vanishes nor diverges at this quantum critical point. However, σ will depend on the critical dynamics since the paramagnon propagator enters the calculation of σ in perturbation theory, see Appendix B. The critical correction to the bare or background conductivity further depends linearly on the leading irrelevant operator, which we denote by u. The latter is related to diffusive electron dynamics and one therefore expects the scale of u to be the same as in the disordered Fermi-liquid theory, namely, $[u] = -(d-2)$.[15] Scaling arguments then suggest a generalized homogeneity law

$$\sigma(t,T,\Omega) = f_\sigma(tb^{d-2}g(\ln b), Tb^d g(\ln b), \Omega b^d g(\ln b), ub^{-(d-2)}) = \text{const} + b^{-(d-2)}\tilde{f}_\sigma(tb^{d-2}g(\ln b), Tb^d g(\ln b), \Omega b^d g(\ln b)). \quad (3.14a)$$

Again, there is a resonance condition that leads to a simple logarithm in the t dependence of σ. This is due to the scale dimension of u being the negative of that of t, modulo logarithmic corrections. As in the case of the density of states, we therefore generalize Eq. (3.14a) to

$$\sigma(t,T,\Omega) = \text{const} + \text{const}\times tg(\ln b)\ln b + b^{-(d-2)}\tilde{f}_\sigma(tb^{d-2}g(\ln b), Tb^d g(\ln b), \Omega b^d g(\ln b)). \quad (3.14b)$$

This scaling relation yields

$$\sigma(0,T,0) = \sigma_0\left[1 + c_\sigma\left\{\frac{T}{T_F}g\left(\frac{1}{d}\ln\frac{\epsilon_F}{T}\right)\right\}^{(d-2)/d} + O(T^{(d-2)/2})\right], \quad (3.15a)$$

and

$$\sigma(t,0,0) = \sigma_0\left[1 + d_\sigma tg\left(\frac{1}{d-2}\ln\frac{1}{t}\right)\ln\frac{1}{t} + O(t)\right], \quad (3.15b)$$

with c_σ and d_σ constants. The same caveat as given after Eq. (3.13b) applies.

An alternative argument that gives Eqs. (3.15) is to assume that σ consists of a background part that does not scale and a singular part, $\delta\sigma$, that does. In fundamental units, $[\delta\sigma] = -(d-2)$. This suggests the scaling form

$$\delta\sigma(t,T,\Omega) = b^{-(d-2)}\tilde{f}_\sigma(tb^{d-2}g(\ln b), Tb^d g(\ln b), \Omega b^d g(\ln b)). \quad (3.16a)$$

Here the dependence on u is already implicitly taken into account, so we dropped the explicit dependence. Taking into account the resonance between the scale dimension of $\delta\sigma$ and t, see Appendix D, gives

$$\delta\sigma(t,T,\Omega) = \text{const}\times tg(\ln b)\ln b + b^{-(d-2)}\tilde{f}_\sigma(tb^{d-2}g(\ln b), Tb^d g(\ln b), \Omega b^d g(\ln b)). \quad (3.16b)$$

This also yields Eqs. (3.15).

The diffusion coefficients D and D_s have dimensions of length squared divided by time. Since there are two time scales, there are two possible scale dimensions for the diffusion coefficients. D_s is the diffusion coefficient for the order-parameter fluctuations so one expects the critical time scale to apply, while D is the quasiparticle diffusion coefficient, so the diffusive time scale is appropriate. This leads to homogeneity laws

$$D_s(t,T,\Omega) = [b^{-(d-2)}/g(\ln b)]f_{D_s}(tb^{d-2}g(\ln b), Tb^d g(\ln b), \Omega b^d g(\ln b)), \quad (3.17a)$$

$$D(t,T,\Omega) = [g(\ln b)]^{-1}f_D(tb^{d-2}g(\ln b), Tb^d f(\ln b), \Omega b^d g(\ln b)). \quad (3.17b)$$

These two results are consistent with the fact that the conductivity is noncritical to the leading order and scales like $\sigma \sim D_s\chi_s \sim DH$. Indeed, the above results for σ, D_s, and D can be used to obtain scaling results for χ_s and $\gamma_C \propto H$, which justify our free-energy considerations in Sec. III B 2 above.

4. Relaxation rates

The phase-breaking rate $\tau_{\rm ph}^{-1}$ and the quasiparticle decay rate $\tau_{\rm QP}^{-1}$ are given by Eqs. (3.4). By comparing Eq. (3.4b)

and Eq. (3.3a), we see that $\tau_{\rm ph}^{-1}$ scales like a wave number squared (recall that G is not singularly renormalized and hence does not scale) and therefore has a scale dimension $[\tau_{\rm ph}^{-1}]=2$ with no logarithmic corrections. This observation leads to the homogeneity law

$$\tau_{\rm ph}^{-1}(t,\epsilon,T)=b^{-2}f_{\rm ph}(tb^{d-2}g(\ln b),\epsilon b^{d}g(\ln b), Tb^{d}g(\ln b),ub^{-(d-2)}). \tag{3.18a}$$

The leading irrelevant variable u represents interaction effects that are necessary for any dephasing. The rate is therefore linear in u, and we can write

$$\tau_{\rm ph}^{-1}(t,\epsilon,T)=b^{-d}\tilde{f}_{\rm ph}(tb^{d-2}g(\ln b),\epsilon b^{d}g(\ln b),Tb^{d}g(\ln b)). \tag{3.18b}$$

At criticality, we find

$$\tau_{\rm ph}^{-1}(0,\epsilon,0)=c_{\rm ph}\epsilon g\left(\frac{1}{d}\ln\frac{\epsilon_{\rm F}}{\epsilon}\right)+O(\epsilon^{d/2}), \tag{3.18c}$$

where $c_{\rm ph}$ is a constant.

The quasiparticle-relaxation rate is given by the ratio H''/H', see Eq. (3.4a). The scaling properties of $\tau_{\rm QP}^{-1}$ thus follow from those of H or γ_C, Eq. (3.9b). Explicitly we find

$$\tau_{\rm QP}^{-1}(t=0,\epsilon,T=0)=c_{\rm QP}\epsilon\ln\left[\ln\frac{\epsilon_{\rm F}}{\epsilon}\right]\Big/\ln\frac{\epsilon_{\rm F}}{\epsilon}+\cdots, \tag{3.19}$$

where $c_{\rm QP}$ is a constant. For $\epsilon\ll\epsilon_{\rm F}$, $t\neq 0$ we have asymptotically

$$\tau_{\rm ph}^{-1}(t,\epsilon)\propto\tau_{\rm QP}^{-1}(t,\epsilon)\propto(\epsilon/t)^{d/2}. \tag{3.20}$$

To obtain Eq. (3.20) we have used the well-known fact that at the disordered Fermi-liquid fixed point the relaxation rates are proportional to $\epsilon^{d/2}$. In terms of our scaling arguments this result is rederived in Appendix E.

IV. DISCUSSION AND EXPERIMENTAL RELEVANCE

This paper completes our discussion of various aspects of the ferromagnetic phase transition in low-temperature disordered itinerant electron systems. We have given the exact solution for the magnetic critical behavior near the quantum phase transition from a paramagnetic metal to a ferromagnetic metal. We have also determined the critical behavior of a number of other relevant physical variables near the transition, in particular, the electrical conductivity and the tunneling density of states. In addition, we have established several connections between previously formulated theories. We conclude with a discussion of the general aspects of our results and their experimental relevance starting with the former.

A. General discussion

One important aspect of the present analysis is the establishment of connections between various theoretical formulations of the quantum-ferromagnetic-transition problem. First, we related our previous nonlocal order-parameter field theory[4] to the local coupled field theory involving both the fermion-density fluctuations and the magnetic order-parameter fluctuations that was formulated in I. The two theories yield the same critical behavior apart from logarithmic corrections to power-law scaling that were missed in Ref. 4 and are correctly given by the coupled local theory. Second, we have unambiguously related earlier work on the disordered interacting electron problem, involving runaway renormalization-group flow, to the quantum ferromagnetic phase transition.[16] This connection was actually made earlier in Ref. 8. However as explained in the Introduction our argument then was not complete. Indeed, even though Ref. 8 correctly obtained the critical behavior, it failed to identify the nature of the phase transition as the ferromagnetic one. In hindsight, this is surprising given that the scaling theory was used to correctly identify the order-parameter exponent $\beta=2\nu$. The problem was that Ref. 8 was formulated solely in terms of fermionic number and spin-density fluctuations at the Fermi surface, so that the behavior of quantities that involve electrons far from the Fermi surface, such as the magnetization, was not obvious. Indeed, we argued that although the above exponent equality was formally valid, the magnetization was actually zero in the ordered phase since the scaling function had a zero prefactor.[17] This argument was incorrect because it failed to take into account that the electrons away from the Fermi surface are also ordering. This, in turn, leads to a nonzero scaling function.

The difficulties interpreting the theory put forward in Ref. 8 notwithstanding, it is very remarkable that this nonlinear sigma-model formulation of the problem yielded the correct result, since it was not geared at all towards describing ferromagnetism. The focus on degrees of freedom near the Fermi surface mentioned above is one reason and another one is the fact that the sigma model is derived by expanding about the paramagnetic-metal fixed point, so it is not obvious why it is capable of describing a critical fixed point. This is actually a general question about sigma models,[18] and the answer is only incompletely known. Indeed, periodically even the capability of the $O(N)$ nonlinear sigma model to qualitatively correctly describe the Heisenberg transition in $d=3$ has been questioned.[19]

The connection between the runaway renormalization-group flow encountered in low orders of a loop expansion and ferromagnetism is particularly interesting in two-dimensional systems because of recent experiments that show either metallic or metalliclike behavior in Si MOSFETs and other materials,[20] and even more recent ones that show that this behavior happens near a quantum phase transition to a ferromagnetic state.[21] The connection between ferromagnetism and two-dimensional (2D) metalliclike behavior is not obvious, but the observation of a ferromagnetic phase in $d=2$ is consistent with our identification of the runaway flow behavior with ferromagnetism. The same connection was more recently made by others.[22] It is also interesting to note that a nearby ferromagnetic phase in disordered systems is favorable to an exotic type of even-parity, triplet superconductivity.[23] After the experimental observation of 2D metallic behavior, this was proposed as a possible explanation.[24] Proposals of superconducting or otherwise ex-

otic phases as the explanation for the observations are bolstered by the conclusion that conventional metallic behavior in a two-dimensional ferromagnetic system is unlikely to occur.[25] Even if the observed metallic or pseudometallic phase is unrelated to superconductivity, the presence of a ferromagnetic phase makes the existence of a triplet superconducting phase nearby more likely.

B. Experimental consequences

Most of the results of the present paper can be directly checked by experiments, at least in principle. For instance, the pressure tuned ferromagnetic transitions observed at very low temperatures in MnSi (Ref. 26) and UGe_2 (Ref. 27) provide examples of systems where the quantum critical point is directly accessible. These experiments were done on very clean samples, where the ferromagnetic transition at low temperatures is of the first order in agreement with theoretical predictions.[28] However, upon introducing quenched disorder one expects the transition to become of the second order,[28] and the current theory to apply.

The critical behavior predicted for the thermodynamic quantities is markedly different from the mean-field exponents predicted by Hertz's theory.[2] For instance, the predicted value of the magnetization exponent in $d=3$, $\beta=2$ with logarithmic corrections is very different from both the mean-field value $\beta_{\rm MF}=0.5$ and the 3D classical Heisenberg value $\beta_{\rm H}\approx 0.37$. One important remark in this context is that the logarithmic corrections will, over any realistically achievable range of t values, mimic a power so that the observed value of β should be expected to be smaller than 2. Similarly, the correlation-length exponent ν will be equal to 1 with logarithmic corrections in $d=3$. However, these exponents may be hard to measure directly, especially near a quantum phase transition that must be triggered by a nonthermal control parameter that is more difficult to accurately vary than the temperature. It is therefore important that the values of the critical exponents are also reflected in the behavior of the tunneling density of states and the electrical conductivity across the transition. Even though these observables do not show any leading critical behavior, the leading corrections expressed in Eqs. (3.13) and (3.15) reflect the values of ν and z, and they should be easier to measure than the critical behavior of, say, the magnetization. For instance, our prediction for the tunneling density of states in $d=3$ is as follows. Far from the transition, it will show the well-known square-root anomaly as a function of the bias voltage that is characteristic of disordered metals.[29] Near the transition, the voltage region that shows the square-root behavior will shrink and outside of it a region of cube-root behavior will appear, until at criticality the behavior is given by the $\epsilon^{1/3}$ behavior shown in Eq. (3.13a). The same discussion applies to the conductivity as a function of temperature, see Eq. (3.15a). Again, the logarithmic corrections to scaling will manifest themselves in a real experiment as an effective power smaller than 1/3.

In this context we also come back to the relative values of the coefficients a_2 and a_{d-2} in Eq. (2.3a). The leading critical behavior is due to the $|\mathbf{k}|^{d-2}$ term whose coefficient is a_{d-2} as can be seen, for instance, from Eq. (B2) in conjunction with Eq. (2.6c). Since $a_{d-2}=O(1/k_{\rm F}l)$, see Eq. (2.3a), this implies that the leading effects will be manifest only for sufficiently strong disorder or if we scale the wave number with the correlation length ξ, for sufficiently large ξ at fixed mean-free path l. Since $a_d=O(1)$, the nonanalytic term will dominate for $\xi\gtrsim l$ or using $\nu=1$, for $t\lesssim 1/k_{\rm F}l$. Typical values of the disorder results in mean-free paths $l\approx 10/k_{\rm F}$. For such a value, our leading results will apply everywhere in the critical region. For less disordered samples, their region of validity will be correspondingly narrower.

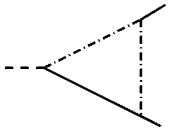

FIG. 9. A one-loop diagram that generates a new three-point vertex. Parts of the diagrams shown in Fig. 2 also contribute to this vertex.

C. Conclusion

In conclusion, we now have a complete theory for the quantum critical behavior of disordered itinerant ferromagnets in $d>2$, including the exact values of the critical exponents, the leading logarithmic corrections to power-law scaling, and the relations between various theoretical approaches to the problem. Specific predictions for the behavior of all important observables allow for a direct experimental test of this theory. However, in $d=2$ there remains a puzzling discrepancy between existing theory and observations. The latest experimental evidence is for a transition with increasing electron density from a paramagnetic insulator to a ferromagnetic metal,[21] while there is no theory that can account for a metallic state, ferromagnetic or otherwise, in $d=2$. In particular, it has recently been shown that ferromagnetic fluctuations in $d=2$ do not produce a metallic state within a perturbative RG treatment[25] ruling out a possible mechanism for a metal-insulator transition in $d=2$. This state of affairs has recently been reviewed in Ref. 20.

ACKNOWLEDGMENTS

Part of this work was performed at the Aspen Center for Physics. We thank the Center for hospitality and E. Abrahams for helpful discussions. This work was supported by the NSF under Grants Nos. DMR-98-70597 and DMR-99-75259.

APPENDIX A: ADDITIONAL THREE-POINT AND FOUR-POINT VERTICES

Starting at one-loop order, the RG generates vertices that are not in the effective action. An example is the three-point vertex shown in Fig. 9.

In contrast to the vertex c_2, all external legs in this diagram carry the same replica index. To see the physical meaning of this term, we integrate out the b field to arrive at an effective four-point q vertex that is completely diagonal in

FIG. 10. One-loop diagrams that generate (a) a two-body and (b) a four-body interaction.

replica space. This corresponds to a four-body interaction term that in imaginary time space must have the form

$$\int_0^\beta d\tau [n_s(\tau)]^4, \tag{A1a}$$

where $n_s(\tau)$ is an electron spin density in imaginary time representation. Performing a Fourier transform and making use of the isomorphism between density operators and q matrices that has been explained in I (see also Ref. 15), this corresponds in schematic notation to

$$T^3 \int d\mathbf{x} \sum_\alpha [Q^{\alpha\alpha}(\mathbf{x})]^4. \tag{A1b}$$

Here $Q(\mathbf{x})$ is the matrix field from I Eq. (2.8) and we have suppressed frequency labels and frequency sums for clarity. A Hubbard-Stratonovich transformation to reintroduce the b-field then leads to a bq^2 vertex of the structure

$$\tilde{c}_2 T^{3/2} \int d\mathbf{x} \sum_\alpha b^{\alpha\alpha}(\mathbf{x}) q^{\alpha\alpha}(\mathbf{x}) q^{\alpha\alpha}(\mathbf{x}), \tag{A2}$$

where $\tilde{c}_2$ is a coupling constant. This vertex thus carries a higher power of the temperature than the one with coupling constant c_2. By using Eqs. (2.11) to estimate the behavior of the diagram shown in Fig. 9 we find that $\tilde{c}_2$ diverges for $d<4$ in the long-wavelength and small-frequency limit, $\tilde{c}_2 = \tilde{\tilde{c}}_2 \Lambda^{d-4}$, where Λ is the infrared-momentum cutoff from Sec. II B 2. The scale dimension of $\tilde{\tilde{c}}_2$ is therefore smaller than that of c_2,

$$[\tilde{\tilde{c}}_2] \leqslant [c_2] - (d-2). \tag{A3}$$

This term is therefore irrelevant for the critical behavior.

Similarly, the RG generates four-point vertices that are not in the effective action. For instance, Fig. 10(a) regenerates the two-body interaction that was shown in I to be irrelevant and was therefore dropped. Figure 10(b) is a four-body interaction of the same type as discussed above in connection with Fig. 9. All of these terms, and similar ones not shown in Fig. 10, are thus RG irrelevant and can be safely neglected.

APPENDIX B: PERTURBATIVE RESULTS FOR THE DENSITY OF STATES AND THE CONDUCTIVITY

In this appendix we show that the scaling results obtained in Sec. III are consistent with perturbation theory for N and σ.

From Eq. (3.1) we find the one-loop result for ΔN as

$$\Delta N(\epsilon_F + \epsilon) = -\frac{N_F}{2} \sum_\beta \sum_m \sum_{i,r} \langle {}^i_r q^{\alpha\beta}_{nm}(\mathbf{x}) {}^i_r q^{\alpha\beta}_{nm}(\mathbf{x}) \rangle_{i\omega_n \to \epsilon + i0}. \tag{B1}$$

Using Eqs. (2.7) and (2.8), this yields

$$\Delta N(\epsilon_F + \epsilon) = \frac{3\pi}{4} G^2 N_F K_t \frac{1}{V} \sum_{\mathbf{p}} T \sum_{m<0} [\mathcal{D}_{n-m}(\mathbf{p})]^2 \times \mathcal{M}_{n-m}(\mathbf{p})|_{i\omega_n \to \epsilon + i0}. \tag{B2}$$

In Sec. II we have seen that the self-consistent one-loop theory for the propagators $\mathcal{D}$ and $\mathcal{M}$ is exact. Using the resulting dressed propagators in Eq. (B2) and doing the integrals, one obtains Eqs. (3.13).

Similarly, if we use the perturbative result for the conductivity given by Eqs. (3.6) of I and the exact propagators derived in Sec. II of the present paper, then Eqs. (3.15) for σ are obtained.

These two results buttress the scaling arguments given in Sec. III. Note that these perturbative calculations are equivalent to taking the standard Altshuler-Aronov perturbative results,[29] and using propagators that are appropriate near the magnetic quantum phase transition.

The classical limit of Eq. (B2) for the density of states or the equivalent result for the conductivity σ can be related to the established result for the critical behavior of the conductivity at a Heisenberg critical point.[30] To see this, note that at finite temperatures the diffusion propagator $\mathcal{D}$ in Eq. (B2) has a mass due to inelastic-scattering processes. For the leading critical behavior, $\mathcal{D}$ can therefore be replaced by a constant. Also, in the classical limit the frequency sum in Eq. (B2) turns into an integral over all frequencies since in this limit the Boltzmann weight that restricts the frequency sum is absent. The net result is that this contribution to ΔN or $\Delta\sigma$ is proportional to a magnetization-magnetization correlation function that is local in space and time,

$$\Delta N \propto \Delta\sigma \propto \langle \mathbf{M}^2(\mathbf{x}, \tau) \rangle. \tag{B3}$$

The correlation function on the right-hand side of Eq. (B3) is essentially the magnetic energy density and hence scales as $t^{1-\alpha}$, t being the distance in *temperature space* to the classical phase transition and α being the usual specific-heat critical exponent. This gives the result of Ref. 30,

$$\Delta N \sim \Delta\sigma \sim t^{1-\alpha}. \tag{B4}$$

APPENDIX C: EQUATION OF STATE

In this appendix we show how to generalize the self-consistent equations given in Sec. II for correlation functions in the paramagnetic phase to the ferromagnetic phase. In this way we will derive and validate the scaling argument given in Sec. III for the magnetization m as a function of t.

To simplify the discussion we first ignore the logarithmic corrections to scaling. Then, in the paramagnetic phase the diffusion coefficient D is simply a number and the equation for D_s is given by Eq. (2.14a) with $D(\omega)$ replaced by that number. The propagators in the ordered phase have been derived in Ref. 25. Assuming that the magnetization is in the z direction, we first need to specify whether longitudinal or transverse spin-density correlations will be considered. In the ferromagnetic phase, the transverse spin-density fluctuations

become propagating Goldstone modes or spin-wave excitations while the longitudinal ones remain diffusive. For the longitudinal spin-density mode, the left-hand side of Eq. (2.14a) therefore still describes a diffusion coefficient. It is easily shown that in this case the diffusion poles on the right-hand side of this equation are cut off by the magnetization. The frequency corresponding to this cutoff is a ''cyclotron'' frequency that scales like $\omega_c \sim |m|$. The explicit generalization of these propagators to the ferromagnetic phase is given by Eqs. (3.10) of Ref. 25. Using these results, the generalization of Eq. (2.14a) to the ferromagnetic phase is, at zero external frequency and wave number

$$D_s = D_s^0 + \frac{iG}{2V} \sum_{\mathbf{p}} \int_0^\infty d\omega \frac{1}{(\mathbf{p}^2 - i\omega/D + c|m|)^2}, \quad \text{(C1)}$$

where c is a constant. Carrying out the integrals yields for $2<d<4$

$$D_s = -c_1|t| + c_2 m^{(d-2)/2}. \quad \text{(C2)}$$

Here $|t| = -t > 0$ is the distance from criticality in the ferromagnetic phase and c_1 and c_2 are constants. Equation (C2) implies that m scales as

$$m \sim |t|^{2/(d-2)}. \quad \text{(C3)}$$

Equation (C3) is consistent with the scaling result for the critical exponent β, Eq. (3.11a), apart from logarithmic terms.

The logarithmic corrections to the exponent β can be understood as follows. As noted in Sec. III B 1, the correlation-length exponent ν has leading logarithmic corrections, while the critical exponent γ does not.[8] Within the integral-equation approach and in the paramagnetic phase, this manifests itself in the following structure of the renormalized paramagnon propagator [see Eqs. (3.5) and (2.17b)]:

$$\mathcal{M}(\mathbf{k}, i\Omega_n) = \frac{1}{t + |\mathbf{k}|^{d-2}/g[\ln(k_F/|\mathbf{k}|)] + |\Omega_n|/\mathbf{k}^2}. \quad \text{(C4)}$$

That is, the term proportional to $|\mathbf{k}|^{d-2}$ carries leading logarithmic corrections, while the term t does not. In Eq. (C4) we have left out all constants for clarity. If one scales the wave vector with the correlation length then this structure produces the logarithmic corrections to the exponent ν. In the ferromagnetic phase, the $|\mathbf{k}|^{d-2}$ nonanalyticity is cut off by a magnetic length or cyclotron radius, $l_m \propto 1/m^{1/2}$. This means that the $|\mathbf{k}|^{d-2}$ gets replaced by $m^{(d-2)/2}$, see Eq. (C2). The net result is that again t has no leading logarithmic correction, while $m^{(d-2)/2}$ does have one. Scaling m with the appropriate power of t then yields Eq. (3.11a) for β.

APPENDIX D: LOGARITHMIC CORRECTIONS TO SCALING

Wegner[31] has given a classification of logarithmic corrections to scaling. The first class consists of simple logarithms that arise due to resonance conditions between scale dimensions. In the present context, such a resonance occurs between the scale dimensions of the leading correction to the single-particle density of states and the relevant variable t. For clarity, let us neglect the more complicated logarithms that are embodied in the function $g(\ln b)$ for the time being. The one-loop flow equations for these two quantities then are

$$\frac{d\Delta N}{d\ln b} = (d-2)\Delta N + \text{const} \times t, \quad \text{(D1a)}$$

$$\frac{dt}{d\ln b} = (d-2)t. \quad \text{(D1b)}$$

The general solution of the homogeneous equation for ΔN is

$$(\Delta N)_{\text{hom}}(b) = (\Delta N)(b=1) b^{d-2}. \quad \text{(D2)}$$

This has the same b dependence as the inhomogeneity $t(b)$. Consequently, the solution of the inhomogeneous equation is

$$(\Delta N)(b) = [(\Delta N)(b=1) + \text{const} \times t(b=1) \ln b] b^{d-2}. \quad \text{(D3)}$$

The resulting logarithm has been taken into account in Eq. (3.12b). [Notice that the physical quantity is $\Delta N(b=1)$.] The same mechanism is at work for the conductivity and this is reflected in Eq. (3.14b).

Wegner's second mechanism is due to marginal operators and it can lead to arbitrary functions of logarithms. In our case, c_2 acts as an effectively marginal operator as has been explained in I and this leads to the log-log-normal factors we denote by $g(\ln b)$.

APPENDIX E: RELAXATION RATES IN A FERMI LIQUID

Here we illustrate how to obtain Schmid's result[32] for the relaxation rates in a disordered Fermi-liquid from the scaling theory developed in Sec. III.

At a disordered Fermi liquid fixed point, the dynamical exponent is $z=2$ reflecting the diffusive dynamics of the quasiparticles, and the leading irrelevant variable, which we denote by u, has a scale dimension $[u] = -(d-2)$.[15] Since $\tau_{\text{ph}}^{-1} \sim \tau_{\text{QP}}^{-1}$ both are dimensionally frequencies or energies they scale the same way and we have for either rate a homogeneity law

$$\tau^{-1}(\epsilon, T) = b^{-2} f_\tau(\epsilon b^2, T b^2, u b^{-(d-2)}). \quad \text{(E1)}$$

The dependence on u arises from the electron-electron interaction terms that lead to $\tau^{-1} \neq 0$ in the first place and therefore the scaling function has the property $f_{\tau^{-1}}(1,0,x) \propto x$. The explicit dependence on u can therefore be eliminated by writing, instead of Eq. (E1),

$$\tau^{-1}(\epsilon, T) = b^{-d} \tilde{f}_\tau(\epsilon b^2, T b^2). \quad \text{(E2a)}$$

In particular, we have[32]

$$\tau^{-1}(\epsilon, 0) = \tilde{f}_\tau(1,0)\epsilon^{d/2}, \quad \text{(E2b)}$$

which we used to derive Eq. (3.20).

[1] D. Belitz, T. R. Kirkpatrick, Maria Teresa Mercaldo, and Sharon L. Sessions, preceding paper, Phys. Rev. B **63**, 174427 (2001).
[2] J. A. Hertz, Phys. Rev. B **14**, 1165 (1976), and references therein.
[3] A. B. Harris, J. Phys. C **7**, 1671 (1974); J. Chayes, L. Chayes, D. S. Fisher, and T. Spencer, Phys. Rev. Lett. **57**, 2999 (1986).
[4] T. R. Kirkpatrick and D. Belitz, Phys. Rev. B **53**, 14 364 (1996).
[5] In clean systems the additional soft modes are ballistic in nature and have a similar effect, see Ref. 6. Although much of our discussion will in general terms apply to clean systems as well, in this paper we will focus on disordered ones.
[6] T. Vojta, D. Belitz, R. Narayanan, and T. R. Kirkpatrick, Z. Phys. B: Condens. Matter **103**, 451 (1997).
[7] For a review, see D. Belitz and T. R. Kirkpatrick, Rev. Mod. Phys. **66**, 261 (1994).
[8] D. Belitz and T. R. Kirkpatrick, Phys. Rev. B **44**, 955 (1991); T. R. Kirkpatrick and D. Belitz, *ibid.* **45**, 3187 (1992).
[9] The values $r=1,2$ correspond to the so-called particle-particle or Cooper degrees of freedom, see Ref. 7. These are not relevant for the discussion of ferromagnetism and therefore have been omitted from the action.
[10] C. Castellani and C. DiCastro, Phys. Rev. B **34**, 5935 (1986).
[11] We use the notation ''$a \sim b$'' for ''a scales like b'' ''$a \approx b$,'' for ''a approximately equals b,'' and ''$a \propto b$'' for ''a is proportional to b.''
[12] More precisely, what is known is that the nonlinear sigma model for the fermionic degrees of freedom, of which the terms of order q^2 and q^4 in Eq. (2.1) are the first two terms in an expansion in powers of q, is renormalizable with two renormalization constants (for G and for H, respectively) *in the absence* of the coupling to the magnetization field M, see, e.g., J. Zinn-Justin, *Quantum Field Theory and Critical Phenomena* (Clarendon Press, Oxford, 1989). The coupling to M amounts to a spin-triplet interaction between the fermions whose interaction amplitude is given by the static paramagnon propagator as can be seen by integrating out M. A standard hypothesis in the theory of interacting disordered electrons is that such a generalized sigma model of interacting fermions is renormalizable as well, albeit with three more renormalization constants (viz., a wave function renormalization and one renormalization constant each for the spin-triplet interaction amplitude and the spin-singlet interaction amplitude that is generated under renormalization), see Ref. 7. There is evidence for this to be true although it has never been proven. If it is true, then the quantities G and H in the second and third terms on the right-hand side of Eq. (2.1) renormalize in the same way. Note that the assumption of all H renormalizing the same way is weaker than that of the interacting sigma model being renormalizable; the latter assumption is sufficient for the former to be true, but not necessary.
[13] D. Belitz, T. R. Kirkpatrick, R. Narayanan, and Thomas Vojta, Phys. Rev. Lett. **85**, 4602 (2000).
[14] H. Fukuyama and E. Abrahams, Phys. Rev. B **27**, 5976 (1983); C. Castellani, C. DiCastro, G. Kotliar, and P. A. Lee, Phys. Rev. Lett. **56**, 1179 (1986).
[15] D. Belitz and T. R. Kirkpatrick, Phys. Rev. B **56**, 6513 (1997).
[16] The history of this subject is intricate and has led to substantial confusion in the literature. A. M. Finkel'stein, Zh. Éksp. Teor. Fiz. **84**, 168 (1983) [Sov. Phys. JETP **57**, 97 (1983)]; Z. Phys. B: Condens. Matter **56**, 189 (1984) first noticed that low-order perturbation theory within a nonlinear sigma model description of disordered interacting electron systems leads, in the absence of any spin-flip processes, to runaway flow; the spin-triplet interaction amplitude flows to infinity at a finite scale. He proposed the formation of local moments as a physical interpretation, A. M. Finkel'stein, Pis'ma Zh. Éksp. Teor. Fiz. **40**, 63 (1984) [JETP Lett. **40**, 796 (1984)]. Attempts to interpret the runaway flow as signaling an unorthodox metal-insulator transition were made by C. Castellani, G. Kotliar, and P. A. Lee, Phys. Rev. Lett. **59**, 323 (1987); T. R. Kirkpatrick and D. Belitz, Phys. Rev. B **40**, 5227 (1989); but these attempts were later shown to be futile by T. R. Kirkpatrick and D. Belitz, *ibid.* **41**, 11 082 (1991). Reference 8 showed that a resummation of the loop expansion to all orders cures the runaway flow problem ruling out the local-moment interpretation and leads to a phase transition that is not, however, a metal-insulator transition. The nature of this transition was correctly recognized in Ref. 4.
[17] See Eq. (4.34) and the accompanying discussion in Ref. 7.
[18] J. Zinn-Justin, *Quantum Field Theory and Critical Phenomena* (Clarendon Press, Oxford, 1996).
[19] See E. Brézin and S. Hikami, cond-mat/9612016 (unpublished), and references therein.
[20] E. Abrahams, S. V. Kravchenko, and M. P. Sarachik, cond-mat/0006055 (unpublished).
[21] S. A. Vitkalov, Hairong Zheng, K. M. Mertes, M. P. Sarachik, and T. M. Klapwijk, cond-mat/0009454 (unpublished).
[22] C. Chamon and E. R. Mucciolo, Phys. Rev. Lett. **85**, 5607 (2000).
[23] T. R. Kirkpatrick and D. Belitz, Phys. Rev. Lett. **66**, 1533 (1991); D. Belitz and T. R. Kirkpatrick, Phys. Rev. B **46**, 8393 (1992); **60**, 3485 (1999).
[24] D. Belitz and T. R. Kirkpatrick, Phys. Rev. B **58**, 8214 (1998).
[25] T. R. Kirkpatrick and D. Belitz, Phys. Rev. B **62**, 952 (2000).
[26] C. Pfleiderer, G. J. McMullan, S. R. Julian, and G. G. Lonzarich, Phys. Rev. B **55**, 8330 (1997).
[27] S. S. Saxena, P. Agarwal, K. Ahilan, F. M. Grosche, R. K. W. Haselwimmer, M. J. Steiner, E. Pugh, I. R. Walker, S. R. Julian, P. Monthoux, G. G. Lonzarich, A. Huxley, I. Sheikin, D. Braithwaite, and J. Flouquet, Nature (London) **406**, 587 (2000).
[28] D. Belitz, T. R. Kirkpatrick, and T. Vojta, Phys. Rev. Lett. **82**, 4707 (1999).
[29] B. L. Altshuler and A. G. Aronov, in *Electron-Electron interactions in Disordered Systems*, edited by A. L. Efros and M. Pollak (North-Holland, Amsterdam, 1985).
[30] M. E. Fisher and J. S. Langer, Phys. Rev. Lett. **20**, 665 (1968).
[31] F. J. Wegner, in *Phase Transitions and Critical Phenomena*, edited by C. Domb and M. S. Green (Academic, New York, 1976), Vol. 6.
[32] A. Schmid, Z. Phys. **271**, 251 (1974).